ACS Catalysis

pubs.acs.org/acscatalysis Research Article

Scope and Mechanistic Investigations of Pd-Catalyzed Coupling/Cyclization and Cycloisomerization of Allenyl Malonates

Logan E. Vine, Ryan D. Reeves, Eleanor M. Landwehr, Israel Fernández,* and Jennifer M. Schomaker*

Cite This: *ACS Catal.* 2021, 11, 9485–9494 Read Online

ACCESS | Metrics & More | Article Recommendations | Supporting Information

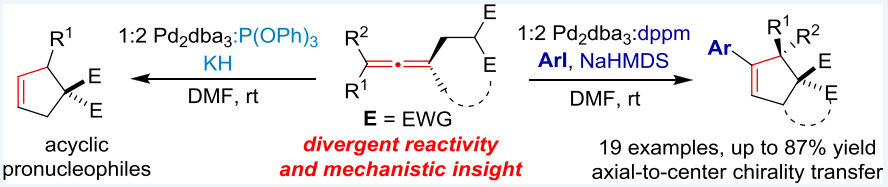

ABSTRACT: Pd-catalyzed transformations of allenyl malonates provide convenient access to functionalized carbocycles, but the influence of the ligand, solvent, base, and reaction conditions on the mechanism, regioselectivity, and product outcome of the cyclization is not well understood. Additionally, from the perspective of synthetic utility, access to either fully substituted or enantioenriched cyclopentane building blocks has not yet been achieved. This work describes how targeted changes to the reaction conditions enable predictable control over the mechanism of Pd-catalyzed allene cross-coupling/cyclization and cycloisomerization, irrespective of the allene substitution pattern. Both enantioenriched cyclopropanes and cyclopentenes can be obtained through axis-to-center chirality transfer from the allene precursor at room temperature, which is not possible using reported Pd-catalyzed methods that result in racemization of the allene. Finally, the ability to divert the reactivity of the allenyl malonate from cross-coupling/cyclization to cycloisomerization by a simple switch of the ligand on Pd from a bidentate phosphine to an electron-poor triphenylphosphite is demonstrated.

KEYWORDS: *allene, carbocyclization, palladium catalysis, cycloisomerization, cyclopentene*

1. INTRODUCTION

Highly substituted cyclopentenes and cyclopentanes are important substructures in a variety of complex natural products and pharmaceuticals (Figure 1).[1] Diverse synthetic methods have been developed to access these cores, including cycloadditions,[2] ring-closing metatheses,[3] Conia-ene cyclizations,[4] and carbonyl-ene[5] cyclizations, among others. However, these strategies differ in the ease with which stereochemical complexity can be introduced into the products. Transition-metal-catalyzed cyclizations of heteroatom-bearing allenes have been studied extensively; however, carbocyclizations of unsaturated precursors, particularly allenes, have been relatively underexplored[6] but offer opportunities for securing rapid access to fully substituted cyclopentanes.

The Cazes group has demonstrated the syntheses of various olefins and dendralenes, albeit in poor selectivities and yields, from the intermolecular reaction of malonates with allenes (Scheme 1A). The groups of Cazes and Ma explored the intramolecular use of allenyl malonates as precursors for the syntheses of cyclopentenes and vinyl cyclopropanes via tandem cross-coupling/cyclization protocols (Scheme 1A).[7] However, the limited scope of this chemistry precluded our efforts to employ it in approaches toward natural products of interest to our group, including jogyamycin and bilobalide, which contain densely substituted cyclopentane cores. Although Ma successfully developed conditions to selectively form cyclopropanes and cyclopentenes from allenes, increasing the substitution on the coupling partner beyond iodobenzene typically reduced the preference for cyclopentene products in favor of cyclopropanes. Only mono- and disubstituted allenes containing no branching were demonstrated to be viable substrates for this chemistry. The product preference was initially hypothesized to arise from the influence of allene substitution on the syn vs anti conformation of a proposed π-allyl intermediate; however, further investigations contradicted this assertion and highlighted our poor understanding of the influence of ligand, solvent, base, and countercation identities on the reaction outcome. Our work presents an in-depth investigation of how factors beyond simple substrate control influence both reactivity and selectivity in Pd-catalyzed cross-coupling/cyclization and cycloisomerization of allenyl malonates. The insights provided by our investigations expand the scope of cross-coupling/cyclizations to encompass trisubstituted allenes and cycloisomerizations of acyclic pronucleophiles to furnish useful synthetic building blocks.

Received: April 22, 2021
Revised: June 28, 2021
Published: July 15, 2021

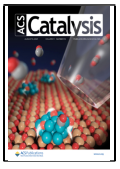

https://doi.org/10.1021/acscatal.1c01847
ACS Catal. 2021, 11, 9485–9494

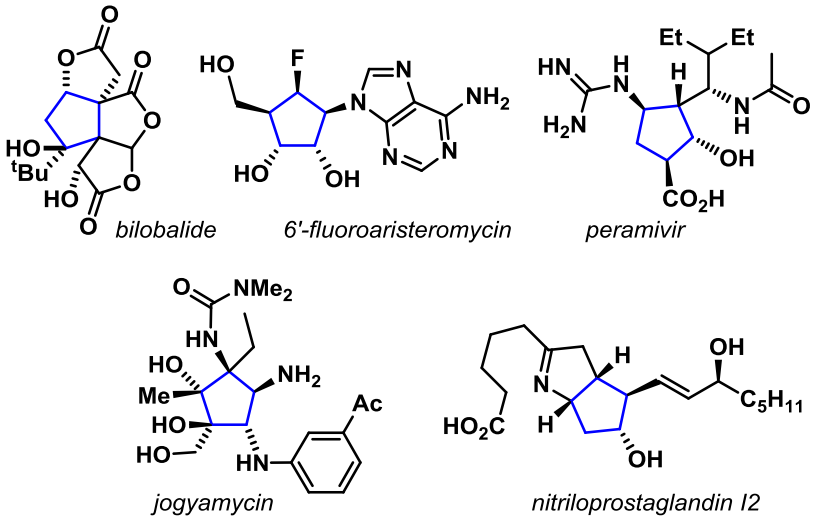

Figure 1. Highly substituted cyclopentanes in drugs and natural products.

Scheme 1. Divergent Pathways for Pd-Catalyzed Reactions of Allenyl Malonates

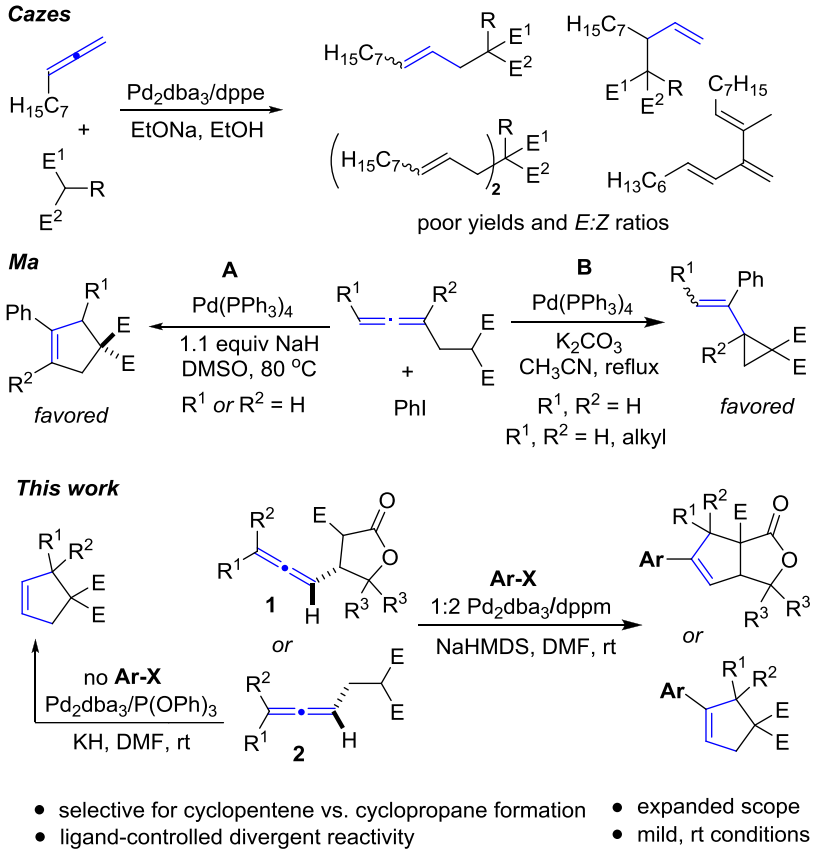

The potential for the asymmetric syntheses of densely substituted cyclopentanes and vinyl cyclopropanes, which were previously unattainable through Pd-catalyzed cyclization of allenyl malonates, is highlighted. The rationale for the observed discrepancies in the reactivities of diverse allene substrates is provided, along with further exploration of the mechanistic details of these chemistries.

2. RESULTS AND DISCUSSION

2.1. Pd-Catalyzed Cross-Coupling/Cyclization of Allenyl Malonates. We began our studies with an investigation of conditions to facilitate the formation of cyclopentene **3a** from allenyl malonate **2a** via a tandem Pd-catalyzed cross-coupling/cyclization sequence. Variations in solvent, temperature, base, and catalyst were carried out to ascertain the trends in reactivity (Table 1). Use of Pd_2dba_3 supported by 1,1-bis-(diphenylphosphino)methane (dppm) in dimethylformamide (DMF) at room temperature (rt) with a variety of bases in DMF (entries 1−5) revealed that bases with a sodium countercation, such as NaHMDS (entries 2 and 3) and NaH (entry 5), gave superior yields. Exploring a series of other common bidentate phosphine ligands in DMF at rt showed that increasing the

https://doi.org/10.1021/acscatal.1c01847
ACS Catal. 2021, 11, 9485−9494

Table 1. Selected Reaction Optimization for Cross-Coupling/Cyclization of 2a to 3a

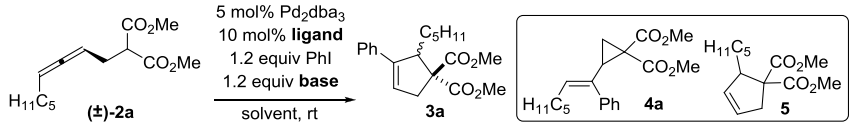

entry[a]	ligand	solvent	base	%3a	2a	4a	5
1	dppm	DMF	LiHMDS	10	49		
2	dppm	DMF	NaHMDS	65			
3	dppm	DMF	NaHMDS[b]	71			
4	dppm	DMF	KHMDS	33			
5	dppm	DMF	NaH	71(67[c])			0
6	dppe	DMF	NaH	38			7
7	dppp	DMF	NaH	51			6
8	dppf	DMF	NaH	44			
9	dppf	DMF[e]	NaH	54			
10	dppf	THF	NaH	0	85		
11	dppf	THF[d]	NaH	52			
12	dppf	DMSO	NaH	trace	70		
13	dppf	DMF	KH	0	44	34	
14	$P(OPh)_3$	DMF	NaH	16	0	0	24
15	$P(p\text{-}CF_3\text{-}Ph)_3$	DMF	NaH	25	0	0	12
16	Me-DuPhos	DMF	NaH	6	83	0	0
17	TangPhos	DMF	NaH	0	93	0	0
18	JOSIPHOS	DMF	NaH	0	83	0	0
19	WALPHOS	DMF	NaH	32	18	0	0
20	(±)-SPANPHOS	DMF	NaH	58	8	0	0

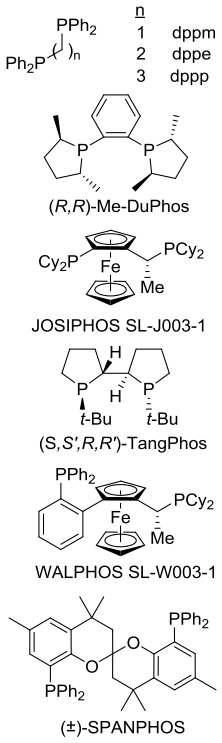

[a]Yields determined by ^1H NMR with Ph_3SiMe as an internal standard. [b]1.0 equiv of base. [c]Isolated yield. [d]Run at reflux. [e]Run at 66 °C.

tether length between the two phosphorus atoms in 1,2-bis(diphenylphosphino)ethane (dppe), 1,3-bis-(diphenylphosphino)propane (dppp), 1,1′-ferrocenediyl-bis-(diphenylphosphine) (dppf), and (±)-SPANPHOS (entries 6−8, 20) gave lower yields of **3a** and in some cases, competing cycloisomerization to **5**. Use of 1,1′-ferrocenediyl-bis-(diphenylphosphine) (dppf) in DMF at 66 °C (entry 9) did improve the yield of **3a** to 54%, compared to 44% at rt (entry 8). Employing tetrahydrofuran (THF) as the solvent with dppf gave no conversion at rt (entry 10), but this could be improved to furnish a 52% yield of cyclopentene **3a** at reflux (entry 11). Switching the solvent to dimethyl sulfoxide (DMSO) with NaH almost entirely shut down the reactivity (entry 12). Interestingly, and in contrast to previous reports[7b] of substrate-controlled regioselectivity, we found that simply switching the base from NaH to KH under the same conditions (compare entries 8 and 13) reversed selectivity from the formation of **3a** to the cyclopropane **4a**, albeit in low yield.

Use of a triaryl phosphite and an electron-poor triaryl phosphine ligand (entries 14 and 15) gave low yields of **3a**, although significant amounts of **5** were noted, where cycloisomerization competes with the desired cross-coupling/cyclization. A series of enantioenriched ligands were attempted, with an eye toward asymmetric cross-coupling/cyclizations (entries 16−19), but the yields of **3a** were significantly lower.

With optimized conditions in hand, the scope was examined with a variety of allenes and coupling partners (Table 2). The electronics of the aryl group had little effect, as electron-poor arenes furnished **3b−g** and **3l** in good yields, while electron-rich arenes delivered **3h−k** in similar yields. The functional group compatibility was excellent; carbonyl-containing groups on the arene, including esters, ketones, and aldehydes were well tolerated, albeit in a decreased yield for **3c**. An aryl bromide gave **3f** with no competing reactivity, highlighting the compatibility of the method with valuable functional handles. Coupling with 3-iodo pyridine and 2-iodothiophene gave **3g** and **3m** in good yield, while the extended π-system of naphthalene gave **3h** in moderate yield. This result, along with **3j−k**, demonstrated a tolerance of the chemistry for ortho-substitution in the iodoarene. A doubly meta-substituted aryl iodide gave a good yield of **3i**; however, iodomesitylene was too hindered and resulted in no reactivity. An aryl iodide containing both a nitro and a chloro substituent provided **3l** in 39% yield.

Variations in the substitution pattern of the allene precursor were also investigated. The 1,1,3-trisubstituted allene **2n** afforded **3n** in 87% yield, the first example of this substitution pattern that does not furnish significant cyclopropane as a byproduct. Addition of a methyl group to the distal allene carbon gave **3o** in 48% yield, the first example of successful cyclopentene formation from an allene bearing a 1,3,3-substitution pattern. Increasing the steric pressure in the allene by replacing C_5H_{11} with an *i*-Bu group required heating the reaction in a sealed vial to give **3p** in 38% yield. Alteration of the bis-ester pronucleophile to an allenyl lactone was also successful. Cross-coupling/cyclization gave **3q** in good yield, while addition of a *gem*-dimethyl group to the lactone ring formed **3r** in 60% yield. Finally, the formation of **3s** in moderate yield showed the

https://doi.org/10.1021/acscatal.1c01847
ACS Catal. 2021, 11, 9485−9494

Table 2. Scope of Allenyl Malonate Cross-Coupling/Cyclization

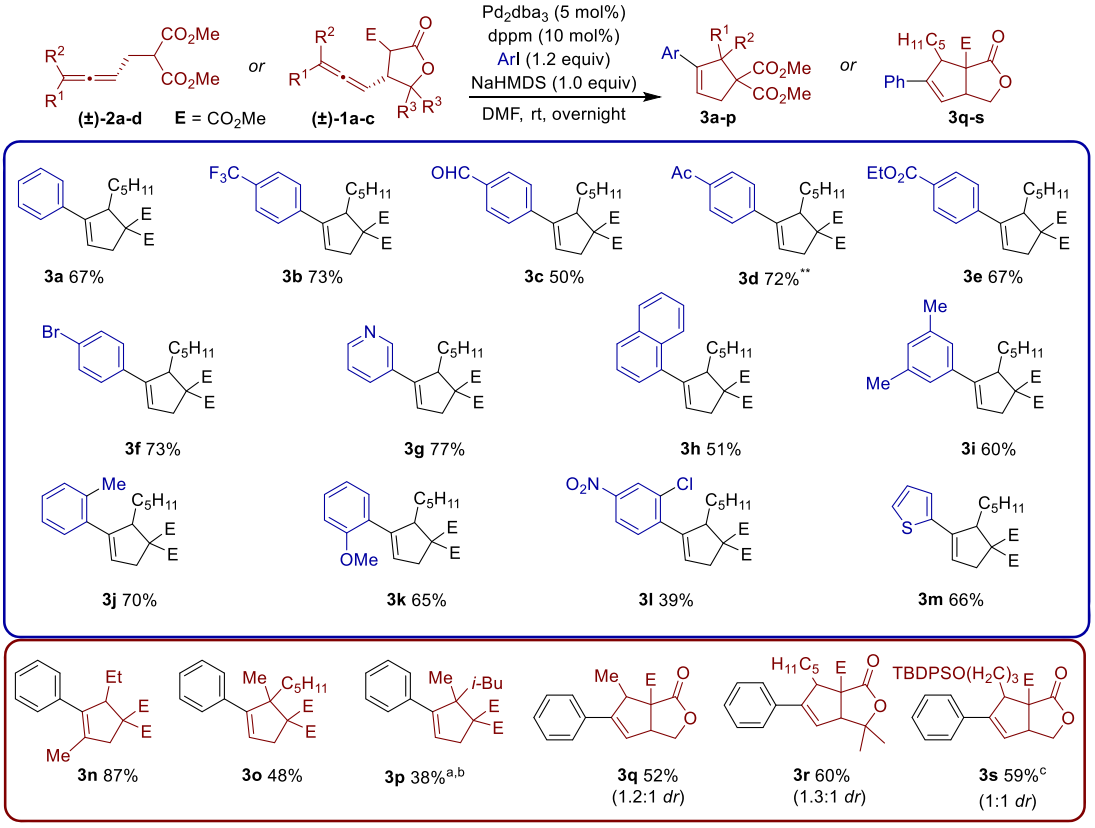

[a]Yield based on isolated mixture of **3r/2a**. [b]run in pressure tube at 66 °C [c]run at 66 °C *NMR yield. **Average NMR yield over 2 runs.

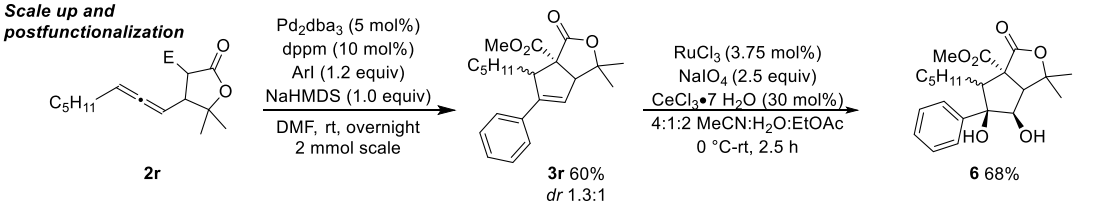

[a]Yield based on isolated mixture of **3p**/**2a**. [b]Run in pressure tube at 66 °C. [c]Run at 66 °C. [d]NMR yield. [e]Average NMR yield over two runs.

tolerance of silyl ethers to the reaction conditions, though the steric demand of TBDMS required increased temperatures.

The methodology was tolerant of a wide variety of functional groups and heterocycles and exhibited mild reaction conditions, with only extremely hindered allenes requiring increased temperatures. These scaffolds are scalable and convenient for the synthesis of fully substituted cyclopentanes, as demonstrated by the 2 mmol scale synthesis of **3r** in 60% yield and subsequent $RuCl_3$-catalyzed dihydroxylation to furnish the cyclopentane **6** in 68% yield and 1.4:1 diastereomeric ratio (dr). In all examples reported in Table 2, the regioselectivity was consistent for the exclusive formation of the cyclopentene, irrespective of the substitution pattern at the distal allene carbon. When this observation is coupled with our studies showing good regioselectivity for cyclopentene formation in precursors with substitution at the proximal allene carbon, previous assertions that regioselectivity depends on the substrate sterics appear unlikely.[7]

3. MECHANISTIC PROPOSAL

Previously proposed mechanisms of Pd-catalyzed cross-coupling/cyclizations of allenes appear inconsistent with our experimental observations.[7c,g] This, coupled with a desire to determine if enantioenriched carbocycles could be secured using this chemistry, prompted us to undertake careful mechanistic studies. Previous proposals[7c,g] (Scheme 2) suggested that the reaction proceeds by oxidative addition of Pd(0) into an aryl halide, followed by coordination of deprotonated **2.1** to the allene to furnish **2.2**. Migratory insertion gives the allylic palladium intermediate **2.3a**, which can potentially isomerize to the Pd(η^3-allyl) complexes **2.4a** and **2.4b**. The anti conformer **2.4a** was proposed to give rise to the cyclopropane **4** (path A), while a bond rotation to produce the syn isomer **2.4b** was surmised to ultimately furnish the desired C4-arylated cyclopentene **3** (path B). We envisaged two alternative pathways, one where intermediate **2.2** undergoes nucleopalladation to **2.6**, with or without prior coordination of the enolate to the Pd catalyst. Subsequent reductive elimination provides product **3** and regenerates the catalyst. Alternatively, the alkyl Pd species **2.3a** cyclizes prior to isomerization via an S_N2 or S_N2' mechanism (depending on the regioselectivity of the migratory insertion) to directly form the desired product **3** (path D). Cyclization of intermediate **2.3a** (path D) was deemed highly unlikely, based on previous computational studies[8] and

https://doi.org/10.1021/acscatal.1c01847
ACS Catal. 2021, 11, 9485−9494

Scheme 2. Potential Mechanisms for Pd-Catalyzed Cross-Coupling/Cyclization[a]

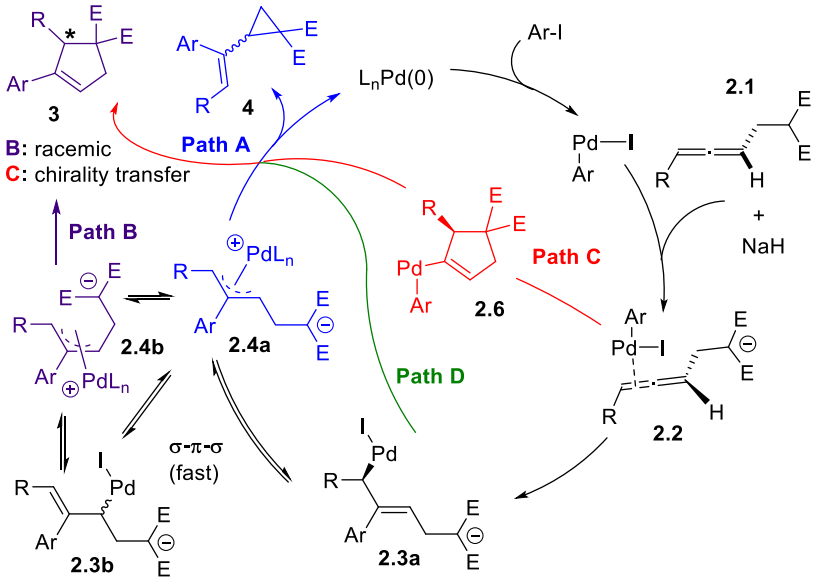

[a]Pd(II) unless otherwise noted.

supporting experimental data indicating that it can undergo facile isomerization to **2.4a** and **2.4b**. We reasoned that a well-designed transfer-of-chirality experiment employing the enantioenriched version of allenyl malonate **2a** could help distinguish between previously proposed paths A and B and the alternative mechanism represented by path C, provided that $\sigma-\pi-\sigma$ isomerization of **2.3a** competes with cyclization.

We found that the chirality in (R_a)-**2a** was transferred to **3** with 98% fidelity (Scheme 3a). Pd(η^3-π-allyl) complexes, such

Scheme 3. Transfer-of-Chirality Experiments

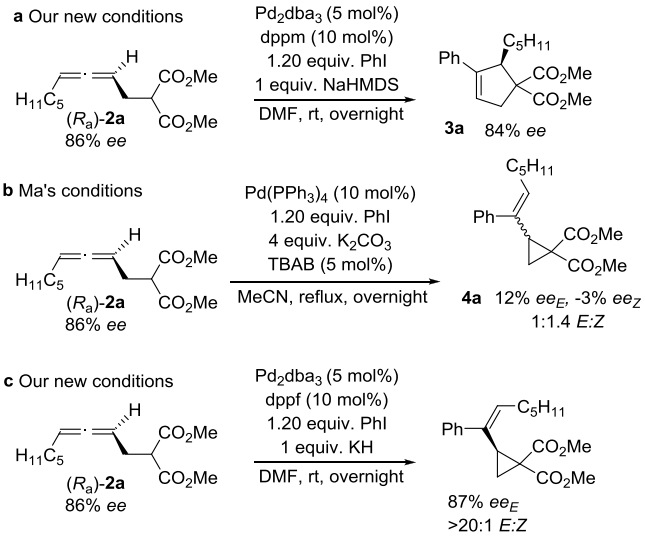

as **2.4a**, have been shown to rapidly interconvert via the intermediate σ-allyl complexes (such as **2.3a** and **2.3b**), resulting in racemization of the allene axial chirality in the product.[6t−v] The presence of such complexes in the catalytic cycle would be expected to lead to significant erosion of enantiomeric excess (*ee*) in transfer-of-chirality experiments. Although path B cannot be definitively ruled out, due to the possibility that cyclization may outcompete racemization, the more likely mechanism is that of the direct nucleopalladation in path C.[6a,9] Path C proceeds by oxidative addition, followed by nucleopalladation to **2.6** and reductive elimination to give the product (**4**), which is consistent with the good observed chirality transfer.

To further support the feasibility of the proposed path C, we computationally explored the formation of the observed cyclopentene **3** (R = CH_3 in the calculations) at the dispersion-corrected PCM(DMF)-B3LYP-D3/def2-TZVP//PCM(DMF)-B3LYP-D3/def2-SVP level (computational details are provided in the Supporting Information).

According to the computed reaction profile (Figure 2), the process begins with the highly exergonic (ΔG_R = −43.4 kcal/mol) oxidative addition of the active Pd(dppm) catalyst to phenyl iodide. This step leads to the formation of the tetracoordinate Pd(II) intermediate **INT1**, a common intermediate for all of the envisaged pathways in Scheme 2, via the transition state **TS1** ($\Delta G^{\neq}$ = 3.3 kcal/mol). Iodide/deprotonated allene **2.1** (R = Me) ligand exchange produces **INT2** in a slightly endergonic step (ΔG_R = 3.0 kcal/mol). Alternatively, the dppm ligand, instead of iodide, might be exchanged by the deprotonated allene reagent. However, the computed high endergonicity of the processes leading to **INT2′** (ΔG_R = 26.6 kcal/mol) or **INT2″** (ΔG_R = 19.0 kcal/mol) makes these alternative ligand exchanges noncompetitive. Similar high endergonicities (ΔG_R = 27.6 and 18.8 kcal/mol, respectively) were also computed when exchanging the Na^+-bonded allene (i.e., the cation interacting with the malonate anion). Neutral intermediate **INT2** then evolves into the cyclic intermediate **INT3** (**2.6** in Scheme 2) via **TS2**, a saddle point associated with the formation of the new C−C bond resulting in the observed five-membered ring. The ease of this carbopalladation/cyclization step is clearly reflected in the low barrier ($\Delta G^{\neq}$ = 5.9 kcal/mol), as well as the high exergonicity (ΔG_R = −21.4 kcal/mol) computed for this cyclization reaction, both of which are fully compatible with the mild room temperature reaction conditions. As shown above (Scheme 2), **INT2** may alternatively undergo a carbopalladation reaction to produce the corresponding intermediate **2.3a** (π-allylpalladium pathway). However, our calculations indicate that this alternative

https://doi.org/10.1021/acscatal.1c01847
ACS Catal. 2021, 11, 9485−9494

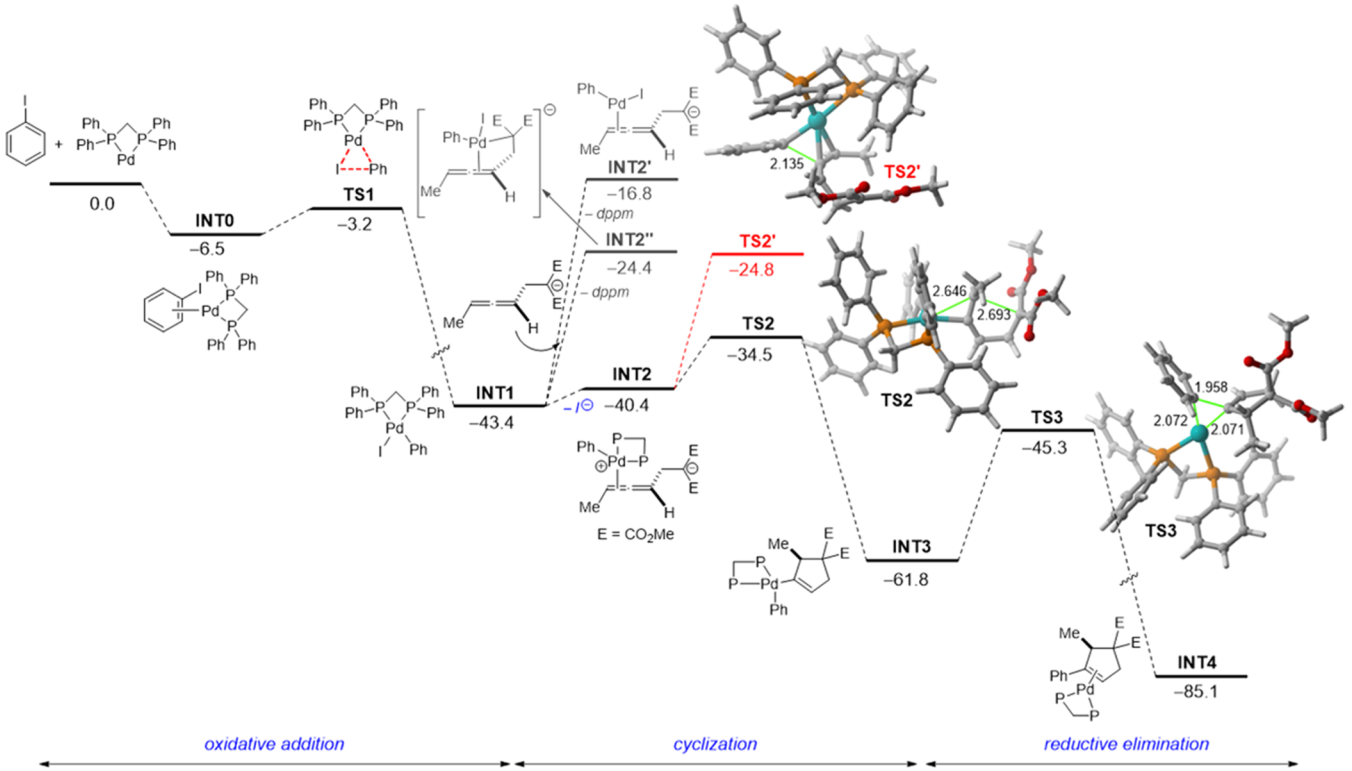

Figure 2. Computed reaction profile for the Pd(0)-catalyzed formation of cyclopentenes. Relative free energies (ΔG, at 298 K) and bond distances are given in kcal/mol and angstroms, respectively. All data have been computed at the PCM(DMF)-B3LYP-D3/def2-TZVP//PCM(DMF)-B3LYP-D3/def2-SVP level.

Scheme 4. Conformational Effects on Product Formation by Conditions

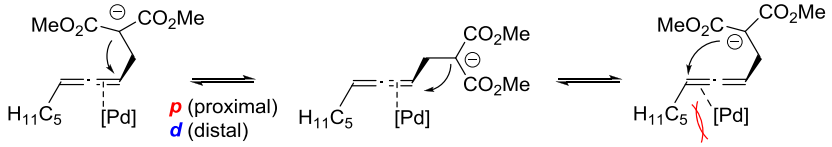

2.2-*p*-syn (from KH, dppf) (access to cyclopropane) | **2.2-*p*-anti (from KH, dppf)** (access to cyclopropane) | **2.2-*d*-syn (from NaH, dppf)** (access to cyclopentene)

pathway can be safely ruled out in view of the much higher barrier required for this step to occur (the corresponding transition state **TS2′**, associated with the formation of the new C−C bond, lies ca. 10 kcal/mol above the preferred **TS2**). **INT3** then undergoes a facile reductive elimination reaction via **TS3** ($\Delta G^{\neq}$ = 16.5 kcal/mol) to produce **INT4**, again in a highly exergonic transformation (ΔG_R = −23.3 kcal/mol). Final decoordination releases the observed cyclopentene **3** (Scheme 2) and the active Pd(0)-dppm catalyst, which can re-enter the catalytic cycle. Therefore, the relatively low barriers and high exergonicities computed for the three steps of the transformation (namely, oxidative addition, cyclization, and reductive elimination) fully support the feasibility of the proposed pathway C under the reaction conditions.

Interestingly, when Ma's cyclopropanation conditions were tested (Scheme 3b), minimal transfer of axial chirality from 86% *ee* (R_a)-**2a** to **4a** was observed, which supports path A for Ma's cyclopropanation conditions. However, when cyclopropanation was observed under our reaction conditions (Table 1, entry 13, vide supra and Scheme 3c), complete transfer of chirality was observed and the opposite stereoisomer to Ma's was formed with excellent *ee*. Although this reaction was not further optimized, it demonstrates that mechanistic understanding can be employed to achieve stereodivergent reactivity.

A rationalization of the results in Scheme 3 should account for experimental observations of the regioselectivity of the reaction based on the reaction conditions. Both the literature and our experimental results demonstrate that regioselectivity can be reversed by changing either the catalyst/base combination[7c,g] or the countercation of the base (Table 1, entries 8 and 13).

We hypothesize that the change in regioselectivity arises from differences in the conformation and nucleophilicity of the intermediate **2.2** (Scheme 4). If we evoke pathway C (Scheme 2) as the preferred mechanism, the first issue to consider is that the cyclopropane can only form when the Pd catalyst is bound to the proximal π-bond (**2.2-*p*-syn** or **2.2-*p*-anti**), while the cyclopentene can only form when the catalyst is bound to the distal π-bond (**2.2-*d*-syn**). The second issue to consider is the difference in the steric environments of the two allene π-bonds. The alkyl substituent at the distal allene carbon will, to some extent, inhibit the coordination of the Pd catalyst to the distal π-bond, due to sterics. The final issue to consider is that the enolate experiences greater stabilization in the presence of a sodium ion, as compared to a potassium ion. The larger dppf-

https://doi.org/10.1021/acscatal.1c01847
ACS Catal. 2021, 11, 9485−9494

Table 3. Optimization of Cycloisomerization of 2a

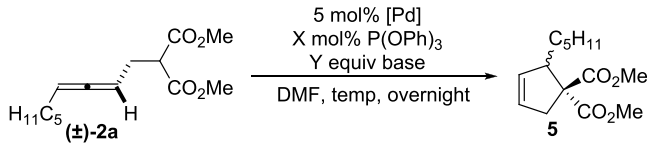

entry	[Pd]	base	equiv	mol % ligand	temp	% yield[a]
1	Pd_2dba_3			10	rt	0 (quant)
2	Pd_2dba_3	NaH	1.2	0	rt	8 (40)
3	Pd_2dba_3	NaH	1.2	10	rt	41 (11)
4	Pd_2dba_3	KHMDS[c]	1.2	10	rt	18 (70)
5	Pd_2dba_3	KHMDS[d]	1.2	10	rt	48 (32)
6	Pd_2dba_3	KHMDS[e]	1.2	10	rt	47 (40)
7	Pd_2dba_3	KH[f]	1.0	10	rt	67[b]
8	Pd_2dba_3	KH[f]	1.2	10	rt	67
9	Pd_2dba_3	KH[f]	0.25	10	rt	53
10	Pd_2dba_3	KH[f,g]	1.0	10	rt	0 (quant)
11	Pd_2dba_3	KH[f]	1.2	5	rt	55
12	Pd_2dba_3	KH[f]	1.2	20	rt	27 (38)
13	$Pd(TFA)_2$	KH[f]	1.0	10	rt	36
14	$Pd(MeCN)_2Cl_2$	KH[f]	1.0	10	rt	trace
15	Pd_2dba_3	KH[f]	1.0	10	0 °C	50 (24)
16	Pd_2dba_3	KH[f]	1.0	10	60 °C	32

[a] ^{1}H NMR yield with $PHSiMe_3$ as an internal standard. Recovered **2a** in parentheses. [b] Isolated yield. [c] 1 M in THF added in one portion. [d] 1 M in THF added over 2 h. [e] 1 M in THF added over 7 h. [f] 50% w/w in paraffin. [g] Substrate and base pre-stirred for 60 min.

ligated catalyst is expected to be more affected by the steric environment of the distal π-bond, as compared to the smaller dppm-ligated catalyst and thus favors coordination to the proximal π-bond, leading to the formation of the cyclopropane product. Additionally, when the less-stabilized potassium enolate serves as the nucleophile, the more strained transition state leading to cyclopropanation becomes accessible (Table 1, entry 13). Interestingly, neither KH/dppm nor NaH/dppf led to any cyclopropanation product.

4. PD-CATALYZED CYCLOISOMERIZATION OF ALLENYL MALONATES

In addition to cross-coupling/cyclization, the direct cycloisomerization of allenyl malonate **2a** to **5** was investigated (Table 3). Interestingly, in our previous work using allenyl lactone substrates, acyclic analogues were completely unreactive in cycloisomerization for reasons that were unclear at the time.[10] The significant presence of **5** in the reaction of **2a** using $P(OPh)_3$ as the ligand (Table 1, entry 14) stimulated efforts to optimize conditions to favor this new transformation (Table 3). A control experiment with no PhI or base (entry 1) gave no **5**, while no ligand resulted in only an 8% yield of **5** (entry 2). Unbound Pd_2dba_3 results in decomposition of **2a**; thus, the correct ligand stoichiometry is essential for good reactivity. The addition of 10 mol % $P(OPh)_3$, in combination with NaH as the base (entry 3), improved the yield of **5** to 41%, with 11% of recovered **2a**. Use of potassium bis(trimethylsilyl)amide (KHMDS) in THF lowered the yield of **5** to 18%, while reducing the addition rate of the base improved the yield to 47−48%, albeit with 32−40% of remaining **2a** (entries 4−6). A dispersion of KH in paraffin at rt (entries 7 and 8) with 10 mol % $P(OPh)_3$ gave the highest observed yields of **5**, presumably due to the slow release of the base during the reaction. Catalytic amounts of KH in paraffin were also effective, as 0.25 equiv of KH gave a 53% yield (entry 9). Again, either lowering or increasing the loading of ligand (entries 11 and 12) had a detrimental effect on yield. Pre-stirring **2a** with KH for 45 min completely shut down the reactivity (entry 10). These experiments indicate that some malonate deprotonation is necessary to initiate the catalytic cycle, but the formation of the enolate alone is not sufficient as excess base is detrimental to the yield. The loss of **2a** to competing pathways is consistent with a noted loss in mass balance to 60−80%, though byproducts could not be characterized. These results suggest that both the neutral and the deprotonated malonate play key roles in the catalytic cycle. To test this hypothesis, 0.2 equiv of malonate **2a** was pre-stirred with base and transferred to a flask containing the catalyst and the remaining 0.8 equiv of **2a**. The desired product **5** was obtained in a 77% yield by NMR, accompanied by 16% of the remaining **2a**, thus supporting key roles for both neutral and deprotonated forms of **2a**. Alternate palladium sources gave diminished or no yield of **5** (entries 13 and 14). Running the reaction at 0 °C (entry 15) gave 50% yield of **5** and moderate mass balance; however, increased temperature reduced the yield of **5** to 32% (entry 16), likely due to increased base availability shutting down the reaction.

The $P(OPh)_3$ is critical for successful cycloisomerization as previous efforts with phosphine-based ligands were unfruitful. $P(OPh)_3$ is a relatively small, monodentate ligand with a Tolman cone angle of 121° and is capable of greater distortion than aryl phosphines, due to the oxygen linker between the P atom and the relatively large phenyl substituent;[11] this decreased steric bulk may promote nucleophilic addition (see Scheme 5, vide infra). Another possibility is that the electron-poor $P(OPh)_3$ furnishes a more electrophilic Pd species that facilitates the cyclization step. One puzzling aspect is the identity of the proton source required to turn over the catalytic cycle. In our previous report of lactone cycloisomerization, the solvent was posited as the proton source, which was supported by deuterium incorporation into the product when CH_3OD was employed.[10] However, the aprotic DMF used in this reaction would require a separate proton source; exogenous water seemed unlikely, given the presence of KH in the reaction.

https://doi.org/10.1021/acscatal.1c01847
ACS Catal. 2021, 11, 9485−9494

Scheme 5. Deuterium Labeling Studies

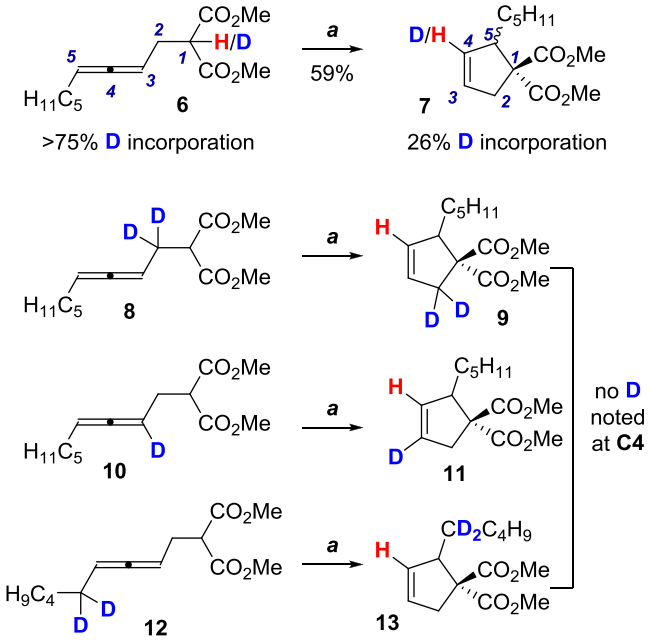

Nevertheless, the reaction was carried out in a glovebox using freshly distilled and degassed DMF and proceeded as normal, ruling out this possibility. Another potential proton source is the acidic proton of the malonate. Oxidative addition of Pd catalysts into acidic C−H bonds, including malonate C−H bonds, to generate nucleophilic species under acidic conditions has been reported by Trost and Ma, among others.[7,12] To test this possibility in our system, allenyl malonate **6** was partially deuterated and the cycloisomerization was carried out under standard conditions (Scheme 5). Partial incorporation of deuterium into **7** was observed, suggesting that the malonate proton can either serve as a proton source or exchange with another proton source in the reaction mixture. Previous reports showing the potential for oxidative formation of a Pd(η^3-allyl) species, in which an allenic or allylic proton is transferred to the palladium center, suggest these sites may be exchangeable. However, the fact that deuterium labeling in **8** and **12** resulted in no D incorporation into C4 of **9** or **13** argued against a mechanism involving this type of intermediate. The possibility of proton exchange at an allenyl C−H bond was ruled out by the lack of incorporation of D at C4 of **11** using deuterium-labeled **10**.

Based on the above data, a catalytic cycle for cycloisomerization is proposed in Scheme 6. The Pd(0) catalyst undergoes oxidative addition into the malonate C−H bond to furnish **5.4**. Separately, deprotonation of the substrate forms the potassium enolate intermediate **5.1**. The Pd(II) intermediate coordinates to the enolate, which undergoes cyclization via nucleopalladation on the distal allene carbon. This furnishes a vinyl palladium intermediate **5.2** that displaces the X-type enolate ligand to regenerate the potassium enolate species. Reductive elimination occurs to give the cycloisomerized product **5.3** and regenerate the Pd(0) catalyst. According to our density functional theory (DFT) calculations (see Figure S1), this proposed pathway is clearly feasible in view of the rather low barriers and high exergonicities computed for the key nucleopalladation ($\Delta G^{\neq}$ = 1.7 kcal/mol, ΔG_R = −26.8 kcal/mol) and subsequent reductive elimination ($\Delta G^{\neq}$ = 2.2 kcal/mol, ΔG_R = −30.6 kcal/mol) steps. Despite this computational support for the nucleopalladation, we cannot rule out the possibility that after **5.1** and **5.4** have formed, **5.4** can undergo a hydropalladation and subsequent isomerization to give a Pd(η^3-allyl) species **5.5**, followed by nucleophilic cyclization to furnish **5.3** and regenerate the Pd(0) catalyst.

5. CONCLUSIONS

In summary, a successful room temperature Pd-catalyzed cross-coupling/cyclization sequence of allenyl malonates was achieved for the regioselective formation of cyclopentenes with challenging substitution patterns. The methodology tolerates a large array of electronically and sterically varied coupling partners, including extended π-systems and heterocycles. The first examples of successful cyclizations of 1,1,3- and 1,3,3-trisubstituted allenyl malonates were reported. Most impor-

Scheme 6. Proposed Mechanism for Cycloisomerization of Allenyl Malonates

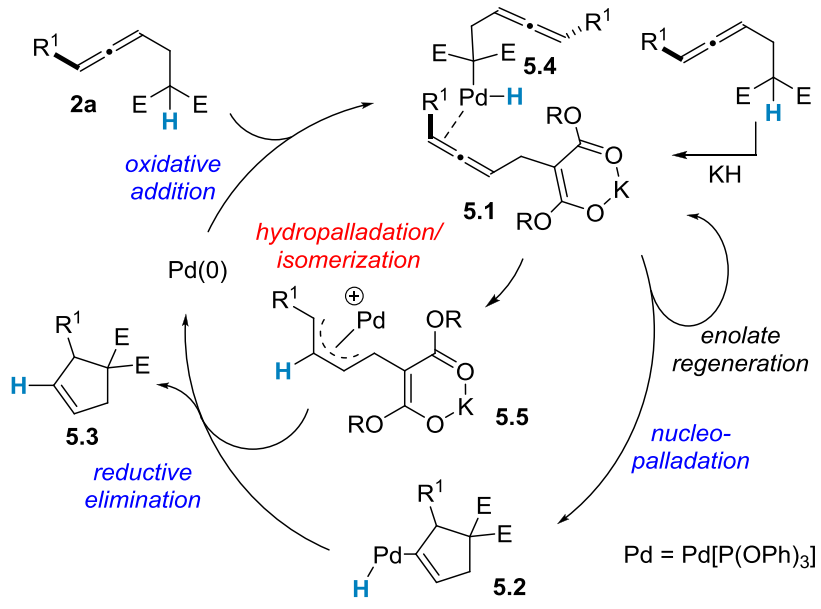

https://doi.org/10.1021/acscatal.1c01847
ACS Catal. 2021, 11, 9485−9494

tantly, this chemistry provides access to enantioenriched cyclopentenes and cyclopropanes via excellent transfer of chirality from the allene precursor to the products. Transfer-of-chirality experiments, coupled with computational support, provide new insights into the mechanism of cross-coupling/carbocyclizations, especially in regard to how divergent mechanisms influence the regioselectivity of the reaction. Switching the ligand on Pd from a bidentate phosphine to an electron-poor triphenylphosphite diverts the reactivity of allenyl malonates from cross-coupling/cyclization to cycloisomerization. Mechanistic studies on the cycloisomerization pathway indicate that the allenyl malonate plays a dual role both as a base and a reactant, promoting an oxidative addition, nucleophilic addition, and reductive elimination sequence to furnish the desired cyclopentenes.

■ ASSOCIATED CONTENT

Supporting Information

The Supporting Information is available free of charge at https://pubs.acs.org/doi/10.1021/acscatal.1c01847.

Characterization data, optimization tables, and additional substrates/catalysts (PDF)

■ AUTHOR INFORMATION

Corresponding Authors

Israel Fernández − *Departamento de Orgánica I and Centro de Innovación en Química Avanzada (ORFEO−CINQA), Facultad de Ciencias Químicas, Universidad Complutense de Madrid, 28040 Madrid, Spain;* orcid.org/0000-0002-0186-9774; Email: israel@quim.ucm.es

Jennifer M. Schomaker − *Department of Chemistry, Madison, Wisconsin 53706, United States;* orcid.org/0000-0003-1329-950X; Email: schomakerj@chem.wisc.edu

Authors

Logan E. Vine − *Department of Chemistry, Madison, Wisconsin 53706, United States*

Ryan D. Reeves − *Department of Chemistry, Madison, Wisconsin 53706, United States*

Eleanor M. Landwehr − *Department of Chemistry, Madison, Wisconsin 53706, United States*

Complete contact information is available at: https://pubs.acs.org/10.1021/acscatal.1c01847

Author Contributions

The manuscript was written through contributions of all authors. All authors have given approval to the final version of the manuscript.

Funding

J.M.S. is grateful to the NIH 1R01GM111412 for the financial support of this research. The Paul Bender Chemistry Instrumentation Center includes Thermo Q Exactive Plus by NIH 1S10 OD020022-1; Bruker Avance-500 by a generous gift from Paul J. and Margaret M. Bender; Bruker Avance-600 by NIH S10 OK012245; Bruker Avance-400 by NSF CHE-1048642; Bruker D8 VENTURE Photon III by NSF CHE-1919350 and the University of Wisconsin—Madison; Varian Mercury-300 by NSF CHE-0342998. I.F. is grateful to the Spanish MICIIN for financial support (grants PID2019-106184GB-100 and RED2018-102387-T).

Notes

The authors declare no competing financial interest.

■ ACKNOWLEDGMENTS

The authors thank Drs. Charles G. Fry and Heike Hofstetter at UW−Madison for their help with NMR techniques and Dr. Martha M. Vestling at UW−Madison for mass spectrometry characterization.

■ REFERENCES

(1) (a) Heasley, B. Recent Developments in the Stereocontrolled Synthesis of Highly Substituted Cyclopentane Core Structures: From Drug Discovery Research to Natural Product Synthesis. *Curr. Org. Chem.* **2014**, *18*, 641−686. (b) Heasley, B. Stereocontrolled Preparation of Fully Substituted Cyclopentanes: Relevance to Total Synthesis. *Eur. J. Org. Chem.* **2009**, *2009*, 1477−1489. (c) Ferreira, A. J.; Beaudry, C. M. Synthesis of natural products containing fully functionalized cyclopentanes. *Tetrahedron* **2017**, *73*, 965−1084.

(2) (a) Moyano, A.; Rios, R. Asymmetric Organocatalytic Cyclization and Cycloaddition Reactions. *Chem. Rev.* **2011**, *111*, 4703−4832. (b) Corbin, J. R.; Ketelboeter, D. R.; Fernández, I.; Schomaker, J. M. Biomimetic Imino-Nazarov Cyclizations via Eneallene Aziridination. *J. Am. Chem. Soc.* **2020**, *142*, 5568−5573. (c) Burrows, L. C.; Jesikiewicz, L. T.; Lu, G.; Geib, S. J.; Liu, P.; Brummond, K. M. Computationally Guided Catalyst Design in the Type I Dynamic Kinetic Asymmetric Pauson−Khand Reaction of Allenyl Acetates. *J. Am. Chem. Soc.* **2017**, *139*, 15022−15032. (d) Grillet, F.; Brummond, K. M. Enantioselective Synthesis of 5, 7-Bicyclic Ring Systems from Axially Chiral Allenes Using a Rh(I)-Catalyzed Cyclocarbonylation Reaction. *J. Org. Chem.* **2013**, *78*, 3737−3754. (e) Brummond, K. M.; Davis, M. M.; Huang, C. F. Rh(I)-Catalyzed Cyclocarbonylation of Allenol Esters to Prepare Acetoxy 4-Alkylidenecyclopent-3-en-2-ones. *J. Org. Chem.* **2009**, *74*, 8314−8320. (f) Han, X.; Wang, Y.; Fangrui, Z.; Lu, Y. Enantioselective [3+2] Cycloaddition of Allenes to Acrylates Catalyzed by Dipeptide-Derived Phosphines: Facile Creation of Functionalized Cyclopentenes Containing Quaternary Stereogenic Centers. *J. Am. Chem. Soc.* **2011**, *133*, 1726−1729. (g) Wilson, J. E.; Fu, G. C. Synthesis of Functionalized Cyclopentenes through Catalytic Asymmetric [3+2] Cycloadditions of Allenes with Enones. *Angew. Chem., Int. Ed.* **2006**, *45*, 1426. (h) Cardoso, A. L.; Soares, M. I. L. 1,3-Dipolar Cycloadditions Involving Allenes: Synthesis of Five-Membered Rings. *Curr. Org. Chem.* **2020**, *23*, 3064−3134. (i) Alcaide, B.; Almendros, P.; Aragoncillo, C. Cyclization Reactions of Bis(allenes) for the Synthesis of Polycarbo-(hetero)cycles. *Chem. Soc. Rev.* **2014**, *43*, 3106−3135. (j) Mascareñas, J. L.; Varela, I.; López, F. Allenes and Derivatives in Gold(I)- and Platinum(II)-Catalyzed Formal Cycloadditions. *Acc. Chem. Res.* **2019**, *52*, 465−479. (k) Trillo, B.; Lopez, F.; Gulías, M.; Castedo, L.; Mascareñas, J. L. Platinum-Catalyzed Intramolecular [4C + 3C] Cycloaddition Between Dienes and Allenes. *Angew. Chem., Int. Ed.* **2008**, *47*, 951−954.

(3) Examples of ring-closing metathesis. (a) Kammerer, C.; Prestat, G.; Gaillard, T.; Madec, D.; Poli, G. Allylic Alkylation and Ring Closing Metathesis in Sequence: A successful Cohabitation of Pd and Ru. *Org. Lett.* **2008**, *10*, 405−408. (b) Widenhoefer, R. A.; Perch, N. S. Silane-Promoted Cycloisomerization of Functionalized 1,6-Dienes Catalyzed by a Cationic (π-Allyl)palladium Complex. *Org. Lett.* **1999**, *1*, 1103−1105. (c) Schmidt, B.; Pohler, M. Tandem olefin metathesis/hydrogenation at ambient temperature: activation of ruthenium carbene complexes by addition of hydrides. *Org. Biomol. Chem.* **2003**, *1*, 2512−2517. (d) Topolovčan, N.; Panov, I.; Kotora, M. Synthesis of 1,2-Disubstituted Cyclopentadienes from Alkynes Using a Catalytic Haloallylation/Cross-Coupling/Metathesis Relay. *Org. Lett.* **2016**, *18*, 3634−3637.

(4) For select reviews see (a) Hack, D.; Blümel, M.; Chauhan, P.; Philipps, A. R.; Enders, D. Catalytic Conia-ene and related reactions. *Chem. Soc. Rev.* **2015**, *44*, 6059−6093. (b) Dénès, F.; Pérez-Luna, A.; Chemla, F. Addition of Metal Enolate Derivatives to Unactivated Carbon−Carbon Multiple Bonds. *Chem. Rev.* **2010**, *110*, 2366−2447. (c) Aubert, C.; Fensterbank, L.; Garcia, P.; Malacria, M.; Simonneau, A. Transition Metal Catalyzed Cycloisomerizations of 1,*n*−Allenynes and Allenenes. *Chem. Rev.* **2011**, *111*, 1954−1993.

(5) (a) Parr, B.; Davies, H. Highly stereoselective synthesis of cyclopentanes bearing four stereocentres by a rhodium carbene-initiated domino sequence. *Nat Commun.* **2014**, *5*, No. 4455. (b) Parr, B.; Li, Z.; Davies, H. Asymmetric synthesis of highly functionalized cyclopentanes by a rhodium- and scandium-catalyzed five-step domino sequence. *Chem. Sci.* **2011**, *2*, 2378−2382. (c) Mikami, K.; Shimizu, M. Asymmetric Ene Reactions in Organic Synthesis. *Chem. Rev.* **1992**, *92*, 1021−1050. (d) Comito, R. J.; Finelli, F. G.; MacMillan, D. W. C. Enantioselective Intramolecular Aldehyde α-Alkylation with Simple Olefins: Direct Access to Homo-Ene Products. *J. Am. Chem. Soc.* **2013**, *135*, 9358−9361.

(6) (a) Ye, J.; Ma, S. Palladium-catalyzed cyclization reactions of allenes in the presence of unsaturated carbon-carbon bonds. *Acc. Chem. Res.* **2014**, *47*, 989−1000. (b) Ma, S. Transition metal-catalyzed/mediated reaction of allenes with a nucleophilic functionality connected to the α-carbon atom. *Acc. Chem. Res.* **2003**, *36*, 701−712. (c) Colby, D. A.; Bergman, R. G.; Ellman, J. A. Rhodium-Catalyzed C−C Bond Formation via Heteroatom-Directed C-H Bond Activation. *Chem. Rev.* **2010**, *110*, 624. (d) Yeung, C. S.; Dong, V. M. Catalytic Dehydrogenative Cross-Coupling: Forming Carbon-Carbon Bonds by Oxidizing Two Carbon-Hydrogen Bonds. *Chem. Rev.* **2011**, *111*, 1215. (e) Yang, B.; Qiu, Y.; Bäckvall, J.-E. Control of Selectivity in Palladium(II)-Catalyzed Oxidative Transformations of Allenes. *Acc. Chem. Res.* **2018**, *51*, 1520−1531. (f) Minehan, T. G. Tandem Bond-Forming Reactions of 1-Alkynyl Ethers. *Acc. Chem. Res.* **2016**, *49*, 1168−1181. (g) Zhu, C.; Yang, B.; Bäckvall, J.-E. Highly Selective Cascade C−C Bond Formation via Palladium-Catalyzed Oxidative-Carbonylation−Carbocyclization−Carbonylation− Alkynylation of Enallenes. *J. Am. Chem. Soc.* **2015**, *137*, 11868−11871. (h) Qiu, Y.; Yang, B.; Jiang, T.; Zhu, C.; Bäckvall, J.-E. Palladium-Catalyzed Oxidative Cascade Carbonylative Spirolactonization of Enallenols. *Angew. Chem., Int. Ed.* **2017**, *56*, 3221−3225. (i) Siebert, M. R.; Osbourn, J. M.; Brummond, K. M.; Tantillo, D. J. Differentiating Mechanistic Possibilities for the Thermal, Intramolecular [2 + 2] Cycloaddition of Allene-Ynes. *J. Am. Chem. Soc.* **2010**, *132*, 11952−11966. (j) Alonso, J. M.; Almendros, P. Deciphering the Chameleonic Chemistry of Allenols: Breaking the Taboo of a Onetime Esoteric Functionality. *Chem. Rev.* **2021**, *121*, 4193−4252. (k) Wang, Q.; Zhang, T.; Fan, Y.; Fan, X. Synthesis of functionalized cyclopentenes through allenic ketone-based multicomponent reactions. *Org. Biomol. Chem.* **2018**, *16*, 8854. (l) Yudha, S. S.; Kuninobu, Y.; Takai, K. Rhenium-Catalyzed Synthesis of Stereodefined Cyclopentenes from beta-Ketoesters and Aliphatic Allenes. *Angew. Chem., Int. Ed.* **2008**, *47*, 9318−9321. (m) Alcaide, B.; Almendros, P. Allenyl-β-lactams: Versatile Scaffolds for the Synthesis of Heterocycles. *Chem. Rec.* **2011**, *11*, 311−330. (n) Alcaide, B.; Almendros, P. Progress in Allene Chemistry. *Chem. Soc. Rev.* **2014**, *43*, 2886−2887. (o) Alcaide, B.; Almendros, P. Gold-Catalyzed Cyclization Reactions of Allenol and Alkynol Derivatives. *Acc. Chem. Res.* **2014**, *47*, 939−952. (p) Alcaide, B.; Almendros, P.; Martínez del Campo, T. Cross Coupling/Cyclization Reactions of Two Different Allenic Moieties. *Chem. − Eur. J.* **2010**, *16*, 5836−5842. (q) Krause, N.; Winter, C. Gold-Catalyzed Nucleophilic Cyclization of Functionalized Allenes: A Powerful Access to Carbo- and Heterocycles. *Chem. Rev.* **2011**, *111*, 1994−2009. (r) Zimmer, R.; Dinesh, C. U.; Nandanon, E.; Khan, F. A. Palladium Catalyzed Reactions of Allenes. *Chem. Rev.* **2000**, *100*, 3067−3126. (s) Marcote, D. C.; Varela, I.; Fernández-Casado, J.; Mascareñas, J. L.; López, F. Gold(I)−Catalyzed Enantioselective Annulations between Allenes and Alkene-tethered Oxime Ethers: A Straight Entry to Highly Substituted Piperidines and Aza-bridged Medium Sized Carbocycles. *J. Am. Chem. Soc.* **2018**, *140*, 16821−16833. (t) Horváth, A.; Backvall, J.-E. Mild and efficient palladium(II)-catalyzed racemization of allenes. *Chem. Commun.* **2004**, 964−965. (u) Kato, F.; Hiroi, K. Stereochemistry of the Asymmetric Carbopalladation of Allenes Followed by Nucleophilic Substitution Reactions with Carbo- and Aminonucleophiles. *Chem. Pharm. Bull.* **2004**, *52*, 95−103. (v) Shi, Z.; Ma, S. Mechanistic switch leading to highly efficient chirality transfer in Pd(0)-catalyzed coupling−cyclization of aryl iodides with 1:1 acid−base salts of 2,3-allenoic acids and L-(−)-cinchonidine or D-(+)-/L-(−)-α-methylbenzylamine. Enantioselective synthesis of highly optically active 3-aryl polysubstituted butenolides. *Chem. Commun.* **2002**, 540−541.

(7) (a) Besson, L.; Goré, J.; Cazes, B. Palladium-catalyzed addition of malonate type compounds to allenes via a hydropalladation process. *Tetrahedron Lett.* **1995**, *36*, 3853−3856. (b) Ma, S.; Jiao, N.; Yang, Q.; Zhang, Z. Highly regio- and stereoselective synthesis of polysubstituted cyclopropane compounds via the Pd(0)-catalyzed coupling-cyclization of 2-(2′,3′-allenyl)malonates with organic halides. *J. Org. Chem.* **2004**, *69*, 6463−6466. (c) Ma, S.; Jiao, N.; Zhao, S.; Hou, H. Control of regioselectivity in Pd(0)-catalyzed coupling-cyclization of 2-(2′,3′-allenyl)malonates with organic halides. *J. Org. Chem.* **2002**, *67*, 2837−2847. (d) Ma, S.; Zhao, S. Reverse of regioselectivity in intramolecular nucleophilic substitution of π-allyl palladium species. Highly selective formation of vinylic cyclopropanes via the Pd(0)-catalyzed coupling-cyclization reaction of organic iodides with 2-(2′,3′-dienyl)malonates. *Org. Lett.* **2000**, *2*, 2495−2497. (e) Bai, T.; Xue, L.; Xue, P.; Zhu, J.; Sung, H.; Ma, S.; Williams, I. D.; Lin, Z.; Jia, G. Insertion reactions of allenes with palladium aryl complexes $[PdI(Ph)(PPh_3)]_2$ and PdI(Ph)(dppe). *Organometallics* **2008**, *27*, 2614−2626. (f) Jiang, X.; Ma, X.; Zheng, Z.; Ma, S. Controllable cyclization reactions of 2-(2′,3′-allenyl)acetylacetates catalyzed by gold and palladium affording substituted cyclopentene and 4,5-dihydrofuran derivatives with distinct selectivity. *Chem. − Eur. J.* **2008**, *14*, 8572−8578. (g) Ahmar, M.; Cazes, B.; Gore, J. Formation De Derives Carbopalladation of β-allenylmalonates: a way to cyclopentenyl or vinylcyclopropyl derivatives. *Tetrahedron Lett.* **1985**, *26*, 3795. (h) Shu, W.; Jia, G.; Ma, S. Palladium-Catalyzed Addition/Cyclization of (2-Hydroxyaryl)-boronic Acids with Alkynylphosphonates: Access to Phosphacoumarins. *Angew. Chem., Int. Ed.* **2009**, *48*, 2788. (i) Bai, W.; Chem, J.; Jia, G. *Comprehensive Organic Synthesis*, 2nd ed.; Elsevier Ltd., 2014; pp 580−647.

(8) (a) Soriano, E.; Fernández, I. Allenes and computational chemistry: from bonding situations to reaction mechanisms. *Chem. Soc. Rev.* **2014**, *43*, 3041−3105. (b) Bai, T.; Ma, S.; Jia, G. Insertion reactions of allenes with transition metal complexes. *Coord. Chem Rev.* **2009**, *253*, 423−448.

(9) (a) Neff, R. K.; Frantz, D. E. Recent applications of chiral allenes in axial-to-central chirality transfer reactions. *Tetrahedron* **2015**, *71*, 7−18. (b) Alonso, J. M.; Quirós, M. T.; Muñoz, M. P. Chirality transfer in metal-catalysed intermolecular addition reactions involving allenes. *Org. Chem. Front.* **2016**, *3*, 1186−1204.

(10) Reeves, R. D.; Kinkema, C. N.; Landwehr, E. M.; Vine, L. E.; Schomaker, J. M. Stereodivergent metal-catalyzed allene cycloisomerizations. *Synlett* **2020**, *31*, 627−631.

(11) Jover, J.; Cirera, J. Computational assessment on the Tolman cone angles for P-ligands. *Dalton Trans.* **2019**, *48*, 15036−15048.

(12) (a) Trost, B. M.; Xu, J.; Schmidt, T. Palladium-catalyzed decarboxylative asymmetric allylic alkylation of enol carbonates. *J. Am. Chem. Soc.* **2009**, *131*, 18343−18357. (b) Trost, B. M. Cyclizations via palladium-catalyzed allylic alkylations. *Angew. Chem., Int. Ed.* **1989**, *28*, 1173−1192.

https://doi.org/10.1021/acscatal.1c01847
ACS Catal. 2021, 11, 9485−9494